Molecular Biology of the Cell
Vol. 20, 3295–3304, July 15, 2009

The Group Migration of *Dictyostelium* Cells Is Regulated by Extracellular Chemoattractant Degradation

Gene L. Garcia,*† Erin C. Rericha,‡ Christopher D. Heger,§ Paul K. Goldsmith,§ and Carole A. Parent*

*Laboratory of Cellular and Molecular Biology, Center for Cancer Research, National Cancer Institute, National Institutes of Health, Bethesda, MD 20892; †Department of Biology, Johns Hopkins University, Baltimore, MD 21218; ‡Institute for Research in Electronics and Applied Physics, University of Maryland, College Park, MD 20742; and §Antibody Production and Purification Unit, Center for Cancer Research, National Cancer Institute, National Institutes of Health, Bethesda, MD 20892

Submitted March 18, 2009; Revised May 8, 2009; Accepted May 15, 2009
Monitoring Editor: Jean E. Schwarzbauer

Starvation of *Dictyostelium* induces a developmental program in which cells form an aggregate that eventually differentiates into a multicellular structure. The aggregate formation is mediated by directional migration of individual cells that quickly transition to group migration in which cells align in a head-to-tail manner to form streams. Cyclic AMP acts as a chemoattractant and its production, secretion, and degradation are highly regulated. A key protein is the extracellular phosphodiesterase PdsA. In this study we examine the role and localization of PdsA during chemotaxis and streaming. We find that *pdsA*$^-$ cells respond chemotactically to a narrower range of chemoattractant concentrations compared with wild-type (WT) cells. Moreover, unlike WT cells, *pdsA*$^-$ cells do not form streams at low cell densities and form unusual thick and transient streams at high cell densities. We find that the intracellular pool of PdsA is localized to the endoplasmic reticulum, which may provide a compartment for storage and secretion of PdsA. Because we find that cAMP synthesis is normal in cells lacking PdsA, we conclude that signal degradation regulates the external cAMP gradient field generation and that the group migration behavior of these cells is compromised even though their signaling machinery is intact.

INTRODUCTION

The process by which cells sense an attractant molecule and respond by migrating directionally toward it is called chemotaxis. Chemotaxis is essential for a variety of physiological processes in mammals as well as for the survival of lower eukaryotes. The mechanisms that regulate the directed migration of neutrophils and *Dictyostelium discoideum* have been extensively studied previously (van Haastert and Devreotes, 2004; Bagorda *et al*., 2006; Friedl and Weigelin, 2008; Stephens *et al*., 2008). One particular challenge of these fast-moving cells is to maintain the ability to respond sensitively and rapidly to an attractant signal. Because both neutrophils and *Dictyostelium* cells use signal relay loops to propagate chemoattractant signals, mechanisms must be at play to maintain detectable levels of chemoattractants. Remarkably, signal degradation also seems to play an important role in the developmental processes of multicellular organisms. Migration of primordial germ cells in *Drosophila* and Zebrafish seems to require degradation of specific lysophospholipids in the former or chemokines in the latter to allow these cells to find their proper developmental environment (Renault and Lehmann, 2006; Minina *et al*., 2007). Many cell types use receptor-mediated degradation to maintain detectable levels of chemoattractants. In this context, cells internalize the bound receptor and as part of the receptor recycling pathway the ligand is released for degradation (Minina *et al*., 2007; Boldajipour *et al*., 2008; Borroni *et al*., 2008; Scola *et al*., 2008). Alternatively, extracellular enzymes can specifically degrade the extracellular signaling molecules, allowing the sensing machinery to go back to basal levels and retain high sensitivity (Leidal *et al*., 2003; Bader *et al*., 2007; Van Lint and Libert, 2007; Leung *et al*., 2008).

Dictyostelium is an excellent model system to study chemotaxis. These social amoebae occur naturally in the soil, and they exist in two independent life stages: a growth stage and a developmental stage (Chisholm and Firtel, 2004; Manahan *et al*., 2004; Mahadeo and Parent, 2006; Urushihara, 2008). On the onset of starvation conditions, the cells enter a developmental program that leads to the aggregation of a group of up to 100,000 cells that eventually form a multicelluar structure. The formation of the aggregate is mediated by the cyclic nucleotide cAMP, which serves as a chemoattractant (Saran *et al*., 2002; Garcia and Parent, 2008; McMains *et al*., 2008). Soon after the onset of starvation, development is initiated by the expression of the adenylyl cyclase A (ACA) and the G protein-coupled cAMP receptor 1 (cAR1) as well as other genes involved in intracellular signaling and sensing of external cAMP (Devreotes, 1994; Parent and Devreotes, 1996; Aubry and Firtel, 1999; Weeks, 2000). Activation of cAR1 leads to the stimulation of a variety of effectors that control chemotaxis, gene expression, and signal relay via the activation of ACA and the secretion of additional cAMP (Parent and Devreotes, 1996; Aubry and Firtel, 1999). Interestingly, as cells form aggregates, they

This article was published online ahead of print in *MBC in Press* (http://www.molbiolcell.org/cgi/doi/10.1091/mbc.E09–03–0223) on May 28, 2009.

Address correspondence to: Carole A. Parent (parentc@mail.nih.gov).

acquire the ability to migrate in groups by aligning in a head-to-tail manner, forming characteristic streams. We have previously shown that the ability of cells to stream depends on the enrichment of ACA-containing vesicles at the back of migrating cells (Kriebel *et al*., 2003, 2008). We propose that the formation of head-to-tail arrays is regulated by the specific release of cAMP from vesicles at the back of cells.

Cyclic nucleotide phosphodiesterases (PDEs), which catalyze the hydrolysis of the 3′-5′ phosphodiester bond, are also up-regulated in early development (Lacombe *et al*., 1986; Bader *et al*., 2007). Four of the seven *Dictyostelium* PDEs degrade intracellular cyclic nucleotides, and the remaining three have extracellular activity (Bader *et al*., 2007). PdsA (also called PDE1 or PdeA) is the main PDE that is responsible for the degradation of extracellular cAMP (Lacombe *et al*., 1986; Bader *et al*., 2007). Cells lacking PdsA show no or greatly reduced extracellular PDE activity and they fail to aggregate under starvation conditions. (Barra *et al*., 1980; Sucgang *et al*., 1997). This phenotype can be rescued by the re-expression of PdsA; however, overexpression leads to aberrant development (Darmon *et al*., 1978; Faure *et al*., 1988, 1989). PdsA has been purified from cells and has been extensively characterized biochemically (Gerisch *et al*., 1972; Brown and Rutherford, 1980; Blondelet and Brachet, 1981; Yamasaki and Hayashi, 1982; Franke and Kessin, 1992). Based upon the presence of PDE activity in cell fractions enriched for membrane, plasma membrane, or both, it has been proposed that PdsA exist in a membrane-bound form and a secreted form (Malchow *et al*., 1972).

Although intracellular signal transduction mechanisms regulating chemotaxis and streaming in *Dictyostelium* have been extensively studied previously (Insall and Andrew, 2007; Janetopoulos and Firtel, 2008; Kay *et al*., 2008; Kolsch *et al*., 2008; Kortholt and van Haastert, 2008), the role that extracellular signal degradation plays in these processes has not been examined. We hypothesize that PdsA, by degrading extracellular cAMP, plays a key role in regulating chemotaxis both by sensitizing the chemoattractant response and by shaping the gradient during streaming. We therefore assessed the role of PdsA in actively chemotaxing *Dictyostelium* cells and determined the cellular distribution of PdsA during chemotaxis. Our data show that extracellular soluble form of PdsA is required for the discrimination and propagation of the cAMP signal during chemotaxis.

MATERIALS AND METHODS

Reagents

Caffeine, ATP, cAMP, dithiothreitol (DTT), and all other reagents were purchased from Sigma-Aldrich (St. Louis, MO) unless otherwise noted. [α-^{32}P]ATP was purchased from MP Biomedicals (Irvine, CA).

Antibodies

Antibodies against ACA (Parent and Devreotes, 1995) and cAR1 (Hereld *et al*., 1994) were a generous gift from Peter Devreotes (Johns Hopkins University, Baltimore, MD). A rabbit polyclonal antibody to PdsA was created against the peptide sequence N-LNDYYTPENWNYYSG-C, corresponding to amino acids 60-74 of the protein sequence. Additional rabbit polyclonal antibodies were generated against three other peptide sequences from the PdsA protein: amino acids 284-298 (N-ANEFPFSVKVKPFEL-C), amino acids 345-358 (N-KQIKIDKLKAIYIE-C), and amino acids 428-443 (N-TQRVIYQQLKEANNNG-C). The specificity of these antibodies was tested using both concentrated extracellular media as well as lysates including both the total cells and the extracellular media. Unpurified and affinity-purified forms of the antisera were tested, and the unpurified serum provided greater sensitivity with little increase in background over the affinity-purified forms. The antibody to amino acids 60-74 was able to detect endogenous levels of PdsA greater than the other antibodies tested. A mouse monoclonal antibody against calnexin (Muller-Taubenberger *et al*., 2001) was obtained from the Developmental Studies Hybridoma Bank maintained by the Department of Biological Sciences at The University of Iowa (Iowa City, IA).

Plasmids, Cell Lines, and Development

The full-length PdsA gene was cloned from genomic DNA isolated from AX3 wild-type (WT) cells by a proteinase K and phenol extraction method adapted from Sambrook (2001). The reverse primer TAGGATCCAATTATTTAAATACAAATTGGATCACCTT and the forward primer AGGATCCTATTAAAAAATGGCATTAAATAAAAAATTGTAAG were used. The polymerase chain reaction (PCR) product was cut using a BamHI and inserted into the BglII site of pB18 (Johnson *et al*., 1991) or pAB3 (reconstructed pCV5 vector) (Janetopoulos *et al*., 2001). The 3′ addition of green fluorescent protein (GFP) or Myc was accomplished by inserting a new restriction site to replace the stop codon (KpnI and ApaI, respectively). This product was inserted into the enhanced GFP (Clontech, Mountain View, CA) or pCMV-Myc (Clontech) vectors and cloned into pB18 or pAB3. For the N-terminal fusions, a mutated full-length gene was amplified to create two pieces with overlapping ApaI restriction sites and a short linker sequence. The N-terminal mutant was formed using the previously mentioned primers and the internal primers CAGTAACGATGGGCCCGGTGGTGGTAGTAATTTTTATAATTTAAATG and CATTTAAATTATAAAAATTACTACCACCACCGGGCCCATCGTTACTG. The Myc epitope or enhanced yellow fluorescent protein (YFP) sequences were inserted in frame into the ApaI site of the N-terminal mutant PdsA gene. Plasmids were electroporated into cells by the method of (Pang *et al*., 1999) by using a MicroPulser electroporation device (Bio-Rad Laboratories, Hercules, CA). Transformed cells were subject to selection with G418 (Geneticin; Invitrogen, Carlsbad, CA) at 2.5–20 μg/ml. Cells were plated on a SM agar plate with a lawn of bacteria and allowed to grow at 22°C (Sussmann, 1966). Plaques that formed fruiting bodies were selected.

Cell lacking PdsA (UK5 and UK7) were obtained from Richard Kessin (Columbia University, New York, NY). In all experiments, UK5 and UK7 cells behaved similarly; for consistency, findings obtained with UK5 cells (which we refer to as *pdsA*$^-$) are presented in this study. WT (AX3) *pdsA*$^-$ or transfected cells were grown in shaking cultures in HL5 media to ~5×10^6 cells/ml and processed for development as described previously (Kriebel *et al*., 2003). Briefly, cells were washed once in development buffer (DB; 5 mM Na_2HPO_4, 5 mM NaH_2PO_4, pH 6.2, 2 mM $MgSO_4$, and 200 μM $CaCl_2$), resuspended in DB at 2×10^7 cells/ml, and shaken at 100 rpm for 4–8 h with pulses of 75 nM cAMP every 6 min. To allow *pdsA*$^-$ cells to develop to the chemotaxis-competent stage, partly purified extracellular media (see below) was also added every 6 min, just after the cAMP pulse. The cells were then processed according to the assay performed.

Partly Purified Extracellular Media

Extracellular media (EC) were partly purified from pdsA/*pdsA*$^-$ cells as described previously, with small modifications (Orlow *et al*., 1981). In brief, cells (4×10^7 cells/ml) were developed for 16 h with 100 nM pulses of cAMP. The cells were removed by centrifugation, and the EC were centrifuged again at 13,000 $\times$ *g* for 30 min (4°C). The EC was subjected to ammonium sulfate precipitation (1.5 M) for 2 h (4°C), centrifuged at 13,000 $\times$ *g* for 30 min (4°C), and the supernatant was retained. Ammonium sulfate precipitation (2.5 M) was carried out again described above. The pellet was resuspended in PDE buffer (50 mM Tris and 10 mM $MgCl_2$, pH 7.5) and placed in a Slide-A-Lyzer dialysis cassette (Pierce Chemical, Rockford, IL) with a 10-kDa permeability limit and dialyzed overnight at 4°C in PDE buffer with 4 mM DTT. The cassette was transferred to PDE buffer with 0.1 mM DTT and dialyzed at 4°C overnight. The solution was removed from the cassette and centrifuged at 48,000 $\times$ *g* for 30 min to remove any insoluble materials. The supernatant was aliquoted and stored at −30°C until use.

Chemotaxis Assays

To examine self-aggregation, cells were developed for 5 h, extensively washed with PB, and plated at 5×10^6 cell/35 mm on plates covered with 1.5% agar in DB. Aggregates and streams were visualized 30 min to 1 h after plating. For assay of the influence of partly purified EC on self aggregation cells, 100 μl of cells was extensively washed and then plated at a density of 5 × 106 cells/ml on eight-well chambered slides (Lab-Tek 155411; Nalge Nunc International, Rochester, NY) and allowed to adhere. The extracellular media were removed and replaced with 200 μl of PB or partly purified EC at given densities. Chemotaxis was visualized using time-lapse microscopy. Under-agarose and micropipette assays were performed as described previously (Parent *et al*., 1998; Comer and Parent, 2006).

Western Blotting

The Crieterion gel system (Bio-Rad Laboratories) was used according to the manufacturer's instructions for all Western blotting. Immunostaining was carried out using standard methods. Transferred membranes were briefly washed in TBS-T (25 mM Tris, 137 mM NaCl, 2.7 mM KCl, pH 7.6, and 0.05% Tween 20) and blocked overnight in either 4% bovine serum albumin in Tris-buffered saline/Tween 20 (TBS-T) (for ACA, cAR1, and Myc) or in 4% nonfat dry milk (for PdsA). Primary antibodies were used at 1:1000 for Myc

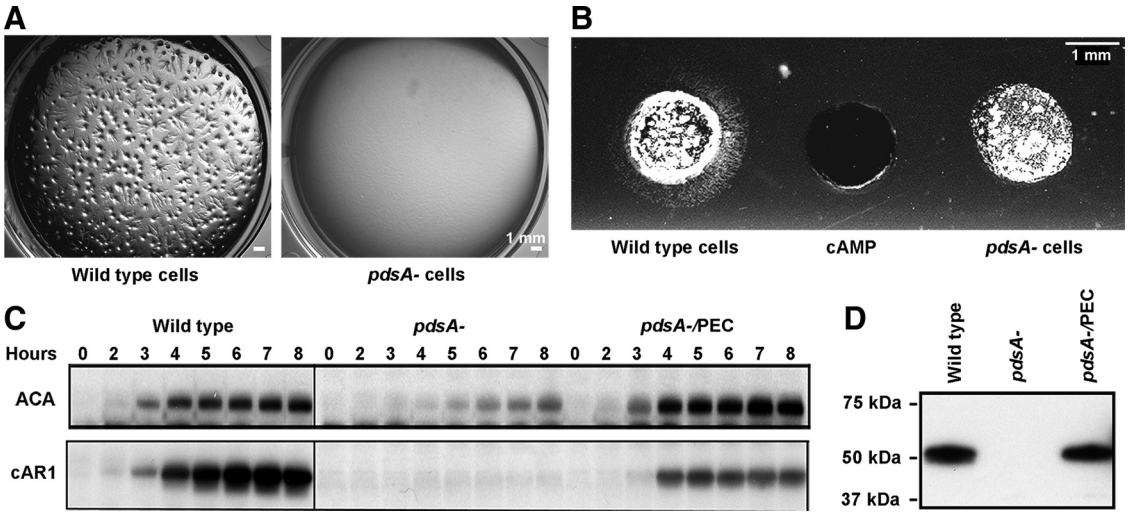

Figure 1. The developmental defect of *pdsA*$^-$ cells can be rescued by exogenously providing partially purified PEC. (A) Cells were pulsed with cAMP for 5 h and plated on nonnutrient agar. Pictures were taken 1 h after plating. Data are representative results obtained from at least three independent experiments. (B) Cells were prepared as described in A and plated into side wells. The center well contains 1 μM cAMP. Images were taken 1 h after plating. Images are representative of at least four independent experiments, each performed in triplicate. (C) Representative Western blot showing the expression pattern of ACA and cAR1 as a function of time after the onset of starvation with exogenous cAMP pulsing. The *pdsA*$^-$ cells developed with PEC (*pdsA*$^-$/PEC) were also provided with an exogenous bolus of PEC slightly after the cAMP pulse (see *Materials and Methods* for details). (D) Representative Western blot showing the amount of PdsA present in the supernatant of *pdsA*$^-$/PEC and WT cells at the 6-h time point.

and PdsA and 1:2000 for ACA and cAR1; secondary antibodies (catalog no. NA934V, horseradish peroxidase [HRP]-linked anti-rabbit and NA931V, HRP linked anti-mouse, GE Healthcare, Chalfont St. Giles, Buckinghamshire, United Kingdom) were used at 1:10,000.

Adenylyl Cyclase Activity Assay

Assay was performed as described previously (Comer *et al*., 2005). Adenylyl cyclase measurements exhibit considerable variation between experiments. From day to day, the amount of labeled ATP decreases due to breakdown of both the isotope and ATP. The most accurate way to compare and display results is by examining the profile and extent of activation between cell lines using the same reaction mix on the same day. Therefore we, and others in the field, have chosen to present adenylyl cyclase activation data as representative of results from at least three independent experiments, each performed in duplicate on a given day.

Fixation and Immunostaining

Developed cells were either plated uniformly on an eight-well chambered slide (Lab-Tek, Nalge Nunc International) and allowed to chemotax for 30 min or plated in 5-μl spots on a two-well chambered slide, overlaid with 1 ml of PB, and subjected to an attractant gradient. Once the cells were polarized and chemotaxing, the buffer was gently removed and replaced with an equal volume of 100% methanol (−20°C). After 5 min, the methanol was replaced with PB and then cells were incubated in blocking solution (10% fetal bovine serum, 2% normal goat serum, and 0.1% digitonin in PB). Fixed cells were washed once with PBS + 0.05% digitonin (PBSD) and then probed with primary antibody in PBSD + 10% blocking solution: rabbit polyclonal anti-Myc (sc-789; Santa Cruz Biotechnology, Santa Cruz, CA) at a dilution of 1:200, mouse monoclonal anti-Myc (sc-40; Santa Cruz Biotechnology) at a dilution of 1:50, mouse anti-calnexin at a dilution of 1:100, or rabbit anti-cAR1 at a dilution of 1:500. After extensive washing, secondary antibody at a concentration of 2 μg/ml in PBSD + 10% blocking solution was added. All secondary antibodies were from Invitrogen (488 goat anti-mouse, 488 goat anti-rabbit, 568 goat anti-mouse, and 555 goat anti-rabbit). Nuclear staining was done with 300 nM 4,6-diamidino-2-phenylindole (D3571; Invitrogen) in PBS for 5 min.

Microscopy and Image Processing

Fluorescent images were taken on a spinning disk confocal microscope (PerkinElmer Life and Analytical Sciences, Boston, MA), micropipette images were taken using either an Axiovert S100 inverted microscope (Carl Zeiss, Thornwood, NY) attached to a MicroPublisher 3.3 RTV camera (QImaging, Surrey, BC, Canada) or Axiovert 200 inverted microscope (Carl Zeiss) attached to a CoolSNAP HQ camera (Roper Scientific, Trenton, NJ) using a 10× objective (Carl Zeiss). Images were taken using an MZ125 upright stereomicroscope (Leica Microsystems, Deerfield, IL) attached to a MicroPublisher 3.3 RTV camera. Images of self-aggregation were taken on a Axiovert 200 microscope using a BioPrecision 2 multiposition stage (Ludl Electronic Products, Hawthorne, NY) automated by iVision software (iVision Software, Omaha, NE). Images were processed using ERS software (PerkinElmer, Boston, MA), ImageJ (National Institutes of Health, Bethesda, MD), or iVision software.

RESULTS

Addition of Conditioned Buffer Rescues the Developmental Defect of pdsA$^-$ *Cells*

It has been established previously that cells lacking PdsA fail to aggregate and differentiate when plated on nonnutrient agar (Barra *et al*., 1980; Sucgang *et al*., 1997). Some mutated cell lines lacking key signaling proteins have been shown to enter development and become chemotactically competent when given exogenous pulses of cAMP (Pitt *et al*., 1992; Insall *et al*., 1994; Bolourani *et al*., 2006). We therefore tested whether *pdsA*$^-$ cells can be driven to enter development by this method. We pulsed cells for 5 h, plated them on nonnutrient agar, and recorded their ability to chemotax and form aggregates. As expected, 60 min after plating, WT cells streamed into aggregates; however, the pulsed *pdsA*$^-$ failed to do so (Figure 1A). Furthermore, the pulsed *pdsA*$^-$ cells were not able to respond to an externally imposed gradient of cAMP and migrate directionally (Figure 1B).

We found that the expression pattern of the developmentally regulated signaling proteins ACA and cAR1 was aberrant in *pdsA*$^-$ cells. Whereas WT cells began to express ACA and cAR1 at 2 h, peaking at 5–6 h, *pdsA*$^-$ cells expressed ACA later and to a much lesser extent than WT cells and the level of cAR1 remained undetectable until 8 h of development (Figure 1C). To rescue the developmental defect of the *pdsA*$^-$ cells, we partly purified the soluble form of PdsA from the EC of *pdsA*$^-$ cells overexpressing full-length PdsA (PdsA/*pdsA*$^-$), which exhibited robust PDE activity, and added it to starving cells. The purity of the EC was examined by western blotting using an antibody to PdsA and by

examining protein levels by silver staining. Western blot analysis of dilutions from the partially purified extracellular medium preparations, hereafter referred to as PEC, showed that a one-fifth dilution of PEC isolated from WT cells (2.4 μg of protein loaded) detected less PdsA than a 1/250 dilution of PEC isolated from PdsA/*pdsA*$^-$ cells (16 ng of protein loaded) (Supplemental Figure S1). The predominant band in PEC isolated from PdsA/*pdsA*$^-$ cells was PdsA, whereas in PEC isolated from WT cells the PdsA was not distinctly visible (and it did not rescue the developmental defect of *pdsA*$^-$ cells; see below). This suggests that the PEC made from overexpressing cells not only contained more PdsA but also contained less contaminants (Supplemental Figure S1). PEC (from PdsA/*pdsA*$^-$) was added to starving *pdsA*$^-$ cells every 6 min just after the cAMP bolus. After 6 h of starvation, the supernatant of developed *pdsA*$^-$ cells had similar amounts of PdsA compared with WT cells (Figure 1D), showing that the amount of PdsA exogenously provided is similar to what WT cells produce. This treatment bypassed the developmental defect of the *pdsA*$^-$ cells. These cells, which will be referred as *pdsA*$^-$/PEC cells, expressed ACA and cAR1 with timing similar to WT cells, although *pdsA*$^-$/PEC cells did express lower levels of cAR1 (Figure 1C). Together, these findings show that the exogenous addition of a PdsA-enriched PEC to *pdsA*$^-$ cells successfully rescues their ability to reach the chemotaxis-competent stage.

pdsA$^-$*/PEC Cells Have Streaming Defects*

We next wanted to assess the role of PdsA during chemotaxis to cAMP. We first used the population-based under-agarose assay to examine the ability of cells to chemotax to various concentrations of cAMP. This assay also provides insight into the ability of cells to relay chemotactic signals to neighboring cells as their migration in streams is readily observable when they align in a head-to-tail manner. Figure 2A shows representative images of WT and *pdsA*$^-$/PEC cells migrating to a subset of cAMP concentrations, and Figure 2B summarizes the response to a broader concentration range of cAMP. The ability of WT cells to migrate directionally and align in a head-to-tail manner was readily observable at cAMP concentrations ranging from 100 nM to 100 μM, although the streaming behavior was weaker at 100 nM cAMP. We envision that this is due to the fact that fewer cells respond to low attractant concentrations and that relay (and streaming) requires a minimum cell density to occur. Indeed, we found that the apparent amount of WT cells remaining in the wells decreased with increasing attractant concentration (Figure 2A). In contrast, *pdsA*$^-$/PEC cells responded to a narrower cAMP concentration range, migrating to cAMP concentrations between 250 nM and 50 μM, and, most remarkably, forming abnormal, very thick streams compared with WT cells.

We next observed the migration behavior of WT and *pdsA*$^-$/PEC cells in response to a micropipette filled with cAMP. Here, again we observed that *pdsA*$^-$/PEC cells respond to a narrower cAMP concentration range. Whereas WT cells sensed and responded to cAMP concentrations ranging from 100 nM to 1 mM, *pdsA*$^-$/PEC cells were responsive from 250 nM to 0.1 mM cAMP (data not shown). Furthermore, the *pdsA*$^-$/PEC cells seemed less polar than WT cells, displaying a more round, less elongated shape. Nevertheless, we found that both WT and *pdsA*$^-$/PEC cells reached comparable chemotactic speeds independently of the amount of cAMP in the micropipette (data not shown) and, not surprisingly, *pdsA*$^-$/PEC and WT cells showed a similar ability to polymerize actin in response to chemoattractant addition, showing the characteristic rapid peak of cortical F-actin accumulation followed by a return to pseudopod-associated staining (Supplemental Figure S2). We also found that under normal plating densities (4×10^4 cells/cm^2), WT cells streamed during chemotaxis at all cAMP concentration tested (Figure 2C; data not shown). However, as we observed with the under-agarose assay, the *pdsA*$^-$/PEC cells exhibited streaming defects during chemotaxis to a micropipette. Interestingly, we found the streaming behavior of the *pdsA*$^-$/PEC cells to be dependant on the cell plating density to a much greater extent than WT cells. At low cell density (2×10^4 cells/cm^2), the migration of WT cells to the back of cells ahead of them was readily visible (Figure 2C and Supplemental Movie 1). In contrast, at similar plating densities, the *pdsA*$^-$/PEC cells migrated toward the needle as individual cells, only occasionally forming short transient groups (Figure 2D and Supplemental Movie 2). At higher densities (6×10^4 cells/cm^2), the *pdsA*$^-$/PEC cells migrated in large and thick groups and did not form the characteristic thin lines of cells observed with WT cells (Figure 2, C and D, and Supplemental Movies 1 and 2). Moreover, the thick lines of *pdsA*$^-$/PEC cells that did form did not extend far beyond the micropipette tip and were transient in nature. Together, these findings establish that PdsA is required for cells to sense a broader range of chemoattractant and for proper streaming during chemotaxis.

PEC Alters the Streaming Behavior of WT and pdsA$^-$*/PEC Cells*

We next attempted to rescue the streaming defect of *pdsA*$^-$/PEC cells. We plated developed cells on a glass cover chamber and added PEC isolated from PdsA/*pdsA*$^-$ cells or PB, gently mixed to final concentrations of between 12 ng and 5.8 μg protein/ml. The movement of cells was then recorded every minute. Whereas WT cells plated with PB showed extensive streaming after 60 min, *pdsA*$^-$/PEC cells were primarily in small groups or as individual cells, although they did migrate throughout the assay. The addition of PEC at 12 ng/ml did not alter the behavior of either WT or *pdsA*$^-$/PEC cells (data not shown). However, the addition of 580 ng/ml PEC remarkably altered the behavior of both cell lines (the addition of 58 and 120 ng/ml PEC gave rise to less robust effects). WT cells formed small clusters of only three or four cells. In contrast, the *pdsA*$^-$/PEC cells moved into extended branched aggregates, reminiscent of streams (Figure 3 and Supplemental Movies 3 and 4). However, this behavior was dependent on the amount of PEC added. Indeed, at higher concentrations of 1.2 and 5.8 μg/ml, both WT cells and *pdsA*$^-$/PEC cells migrated without streams and formed small aggregates (data not shown). Together, these data show that the ability of cells to properly relay signals and stream is tightly regulated by the presence of PdsA.

Activation and Cellular Distribution of ACA Is Normal in pdsA$^-$*/PEC Cells*

The ability of cells to activate ACA and to secrete cAMP is essential for signal relay and streaming. To determine the mechanism by which PdsA regulates streaming, we assessed the integrity of the ACA signaling cascade in *pdsA*$^-$/PEC cells. In *Dictyostelium*, the signaling cascade from chemoattractant receptors to ACA is highly regulated, requiring inputs from G$\beta\gamma$-subunits, phosphatidylinositol 3-kinase, cytosolic regulator of adenylyl cyclase (CRAC), and target of rapamycin complex 2. The exogenous addition of chemoattractants to whole cells leads to a rapid burst in ACA activity followed by a characteristic slow return to basal levels. We found that the activation of ACA in *pdsA*$^-$/PEC cells is

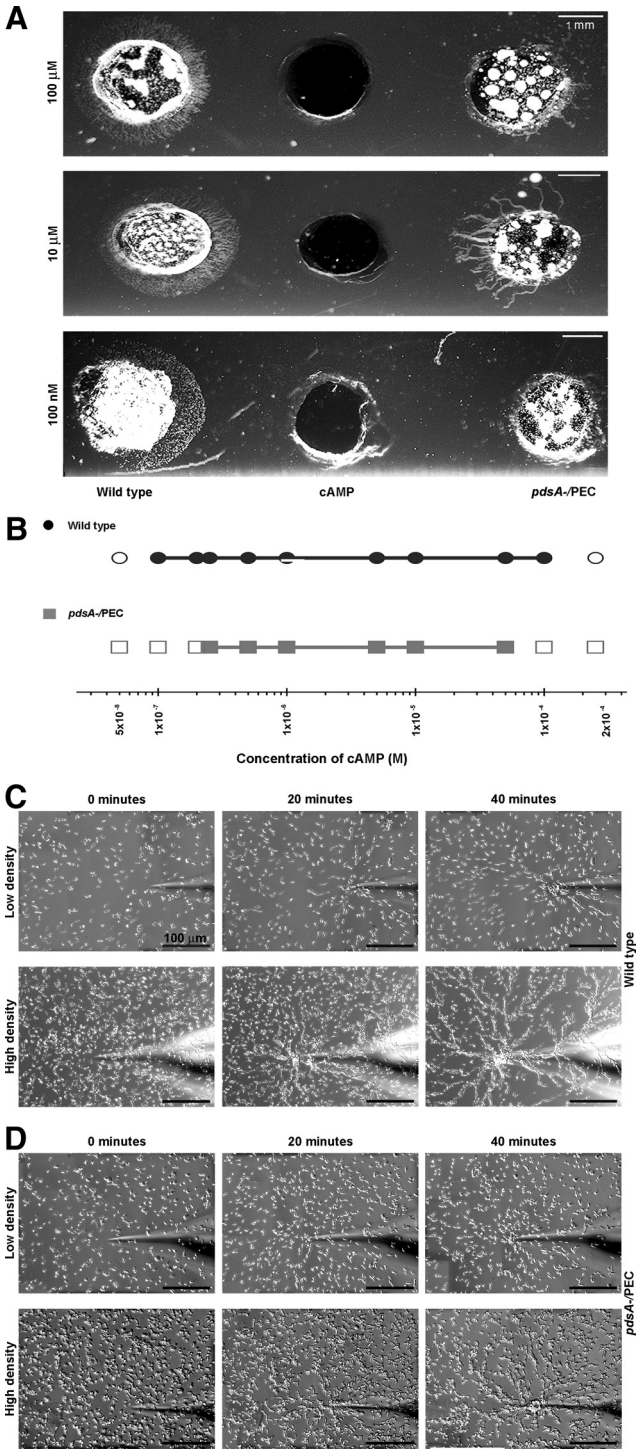

Figure 2. *pdsA*$^-$/PEC cells migrate to a cAMP source but exhibit streaming defects. (A) WT and *pdsA*$^-$/PEC cells were plated into side wells. The center well contains [cAMP] as indicated on the left. Images were taken 1 h after plating. Images are representative of at least four independent experiments, each performed in triplicate. (B) Graph depicting the ability of WT and *pdsA*$^-$/PEC cells to respond chemotactically in the under-agarose assay. The solid circles/lines represent [cAMP] range where cells are able to respond to cAMP; open circles represent [cAMP] that did not elicit a chemotactic response. Ranges were determined from at least three independent experiments. (C and D) Images of WT and *pdsA*$^-$/PEC cells migrating to a micropipette filled with 100 μM cAMP at low and high cell density, as indicated. Images are representative of at least three independent experiments. Also see Supplemental Movies 1 (WT) and 2 (*pdsA*$^-$/PEC cells).

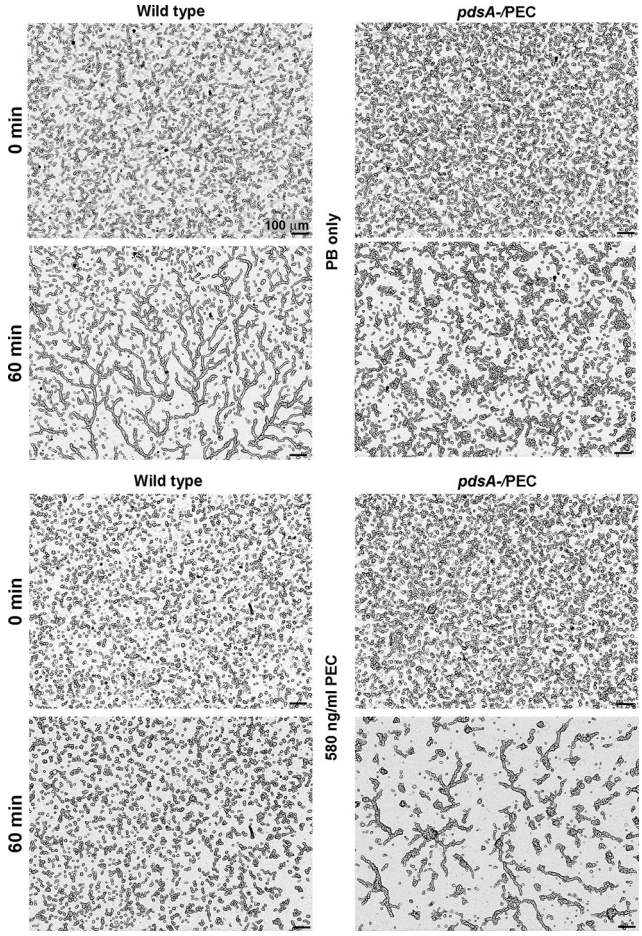

Figure 3. PdsA regulates self-aggregation. Images showing the ability of WT and *pdsA*$^-$/PEC cells to self-aggregate after they are plated at high density. Cells were allowed to reach the chemotaxis-competent stage as described in *Materials and Methods*, plated on a glass chambered slide, allowed to adhere, and overlaid with either PB or PEC diluted in PB to 580 ng protein/μl. Images are representative of at least three independent experiment. Also see Supplemental Movies 3 (WT) and 4 (*pdsA*$^-$/PEC).

similar to WT cells (Figure 4A). These findings establish that PdsA is not required for signals to be properly transduced from chemoattractant receptors to ACA.

Because the enrichment of ACA at the back of migrating cells is also required for cells to migrate in a head-to-tail manner, we transfected *pdsA*$^-$ cells with our ACA-YFP expression plasmid (Kriebel *et al.*, 2003) and assessed the cellular distribution of ACA during chemotaxis and streaming. To further characterize the behavior of *pdsA*$^-$/PEC cells, we also monitored the distribution of the cAMP receptor cAR1-GFP and CRAC-GFP, a pleckstrin homology domain-containing protein necessary for ACA activation and development, in these cells during chemotaxis. We found that, much like in WT cells, cAR1-GFP is uniformly distributed on the plasma membrane in polarized and migrating *pdsA*$^-$/PEC cells as well as in *pdsA*$^-$ cells developed in the absence of PEC (Figure 4B). Likewise, CRAC-GFP is redistributed sharply to the leading edge of polarized and migrating WT and *pdsA*$^-$/PEC cells (Figure 4B). Finally, we also determined that ACA-YFP is highly enriched at the back of these cells, much like in WT cells (Figure 4B). As expected, we found that neither CRAC-GFP nor ACA-YFP exhibited a

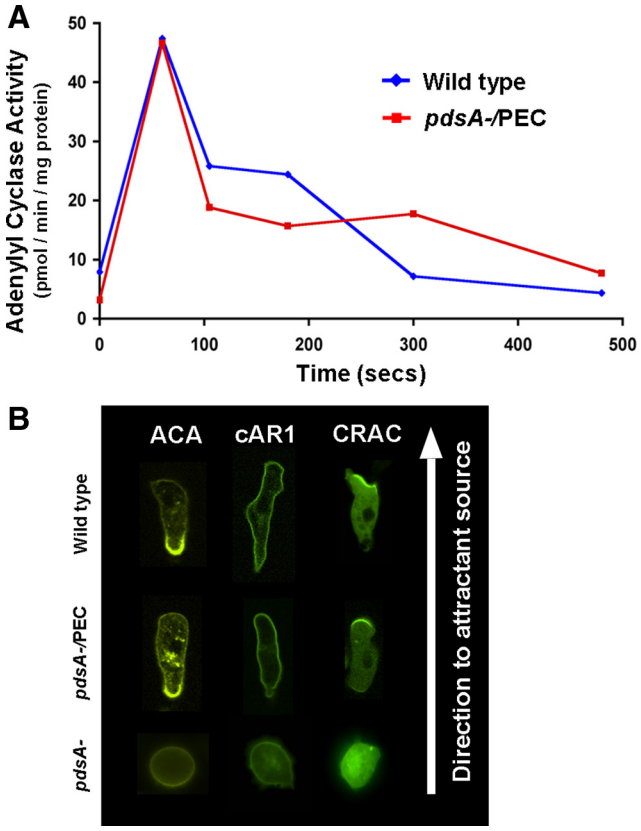

Figure 4. Activation and cellular distribution of ACA is normal in *pdsA*$^-$/PEC cells. (A) Graph depicting the chemoattractant-mediated activation of ACA in WT and *pdsA*$^-$/PEC cells. Cells were stimulated with 10 μM cAMP. Data are representative results from three independent experiments, performed in duplicate. (B) Confocal fluorescent images showing the cellular distribution of ACA-YFP, cAR1-GFP, or CRAC-GFP in WT, *pdsA*$^-$/PEC, and *pdsA*$^-$ cells exposed to a gradient of chemoattractant. The position of the micropipette is at the top of the images. Images are representative of at least three independent experiments.

specific redistribution in *pdsA*$^-$ cells developed in the absence of added PEC (Figure 4B). These findings establish that the presence of PdsA is not required for cells to adequately transduce signals to ACA. Nor is it required for signaling molecules to be properly distributed during chemotaxis and streaming.

PdsA Localizes to the Endoplasmic Reticulum (ER) during Chemotaxis

We next set out to determine the cellular distribution of PdsA during chemotaxis. We constructed YFP fusions at either the C or N terminus of PdsA (PdsA-YFP and YFP-PdsA) and used the phenotypic rescue of cells lacking PdsA as a readout for function of the fusion protein. Whereas the expression of PdsA-YFP failed to rescue the developmental defect of *pdsA*$^-$ cells, YFP-PdsA was able to do so showing characteristic fruiting body formation (Supplemental Figure S3). We developed the YFP-PdsA/*pdsA*$^-$ cells to the chemotaxis-competent stage, exposed them to a micropipette containing cAMP, and studied the cellular distribution of YFP-PdsA. We found a dim YFP signal associated with densely packed intracellular structures that did not colocalize with mitochondria or lysosomes (Supplemental Figure S4). Unfortunately, the YFP-PdsA fusion protein was expressed at low levels making it difficult to clearly follow its distribution in live cells. Furthermore, the expression of YFP-PdsA was quickly lost despite constant antibiotic selection, suggesting that the bulky YFP tag renders the protein unstable.

Because the fluorescently tagged PdsA was unstable, we attempted to visualize the cellular distribution of the endogenous protein by using polyclonal antibodies against PdsA. Although a few of them worked very well for Western analyses (see *Materials and Methods* for details), none worked for immunofluorescence. We therefore tagged PdsA with the Myc epitope (MASMQKLISEED) on either the C or N terminus of the protein. We found that both constructs (Myc-PdsA and PdsA-Myc) rescue the developmental defect of *pdsA*$^-$ cells and that rescued cell lines maintained constant expression levels. By adjusting the concentration of antibiotic during selection, we were able to control the expression level of the Myc-tagged proteins and found that cells given 2.5 μg/ml G418 (G2.5) express PdsA-Myc protein at levels similar to either WT or *pdsA*$^-$/PEC cells (Figure 5A). Interestingly, although the antibody to PdsA was able to detect high levels of Myc-PdsA, the Myc antibody did not strongly detect the Myc-PdsA protein by either Western analysis or immunofluorescence. The epitope recognized by the PdsA antibody is nine amino acids downstream of the insertion site of the N-terminal Myc epitope. Whether the recognition of the Myc antibody is masked by the location of the epitope or the recognition of the PdsA antibody is enhanced by the Myc epitope is unclear. Because the PdsA-Myc protein was strongly detected by the Myc antibody and expressed at a similar level than the WT protein, we used the G2.5 PdsA-Myc/*pdsA*$^-$ cells for further immunofluorescence analyses.

To examine the cellular distribution of PdsA-Myc, we rapidly fixed actively chemotaxing cells with 100% methanol and processed the samples for immunostaining. As we observed for YFP-PdsA, we found the Myc signal to strongly label densely pack intracellular structures that resemble ER (Figure 5B). Indeed, we observed a perfect colocalization signal when we costained with an antibody against calnexin, an ER-specific type I transmembrane protein (Muller-Taubenberger *et al*., 2001) (Figure 5B). Interestingly, we found the PdsA-Myc signal to be specifically excluded from the perinuclear ER pool. Because biochemical studies have suggested that PdsA is associated with the plasma membrane, we set out to determine whether PdsA-Myc localized to the plasma membrane. We used an antibody against cAR1 to visualize the plasma membrane in PdsA-Myc/*pdsA*$^-$ cells and looked for costaining with Myc. We found no colocalization of PdsA-Myc with the plasma membrane (Figure 5C). Although we cannot rule out that the cellular distribution we observe relies on tagged versions of PdsA, the fact that we see a similar distribution using YFP-PdsA or PdsA-Myc, and, more importantly, that both fusion proteins rescue the developmental phenotype of *pdsA*$^-$ cells, strongly argues against a nonspecific effect of Myc or YFP. Together, our findings show for the first time that PdsA is closely associated with the ER during chemotaxis. Furthermore, our studies establish that PdsA is not associated with the plasma membrane during chemotaxis.

DISCUSSION

In this study, we show that chemoattractant degradation is essential for cells to optimally sense external chemical gradients. We show that cells lacking PdsA can reach the chemotaxis-competent stage by exogenously providing PdsA during development. These *pdsA*$^-$/PEC cells are able to migrate directionally to an exogenous gradient of cAMP and

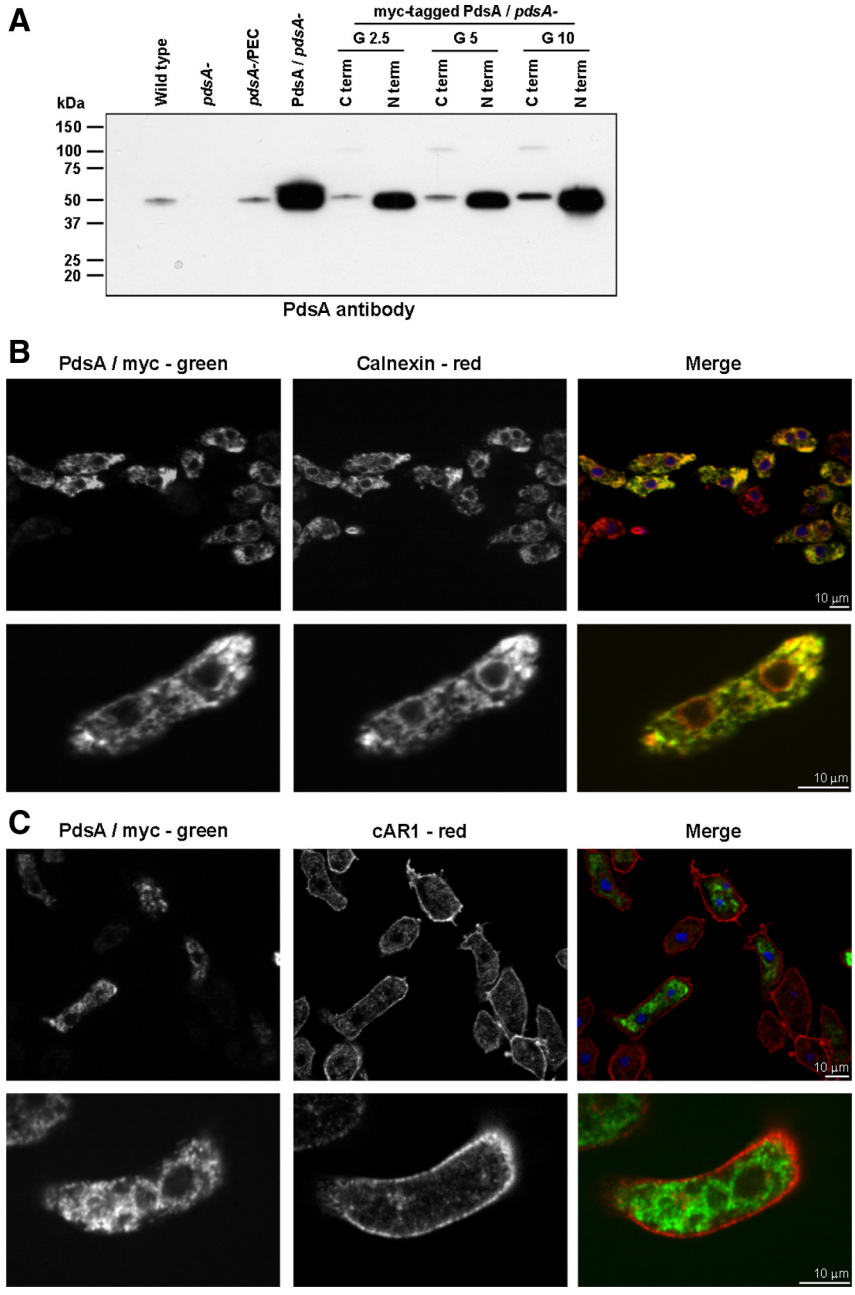

Figure 5. PdsA-Myc localizes to the endoplasmic reticulum. (A) Representative Western blot showing the expression of PdsA, Myc-PdsA, or PdsA-Myc in the supernatant of cells starved and pulsed with cAMP for 5 h. (B and C) Confocal fluorescent images of PdsA-Myc/*pdsA*$^-$ cells fixed and stained for Myc and calnexin (B) or Myc and cAR1 (C). Cells were developed with pulses of cAMP, plated on glass coverslips, and allowed to chemotax before fixation. Images are representative of at least four independent experiments.

show normal, robust polarized F-actin assembly. As expected, we found that *pdsA*$^-$/PEC cells migrate directionally to a narrower range of chemoattractant concentration gradients. We reasoned that when exposed to high cAMP concentration gradients, the receptors become quickly saturated, and the cells cannot sense any difference between their front and back. In contrast, at low cAMP concentration gradients, the *pdsA*$^-$/PEC cells cannot distinguish the exogenously applied stimulus from the endogenous cAMP they produce and they do not respond chemotactically. However, we were surprised to find that the *pdsA*$^-$/PEC cells still show a significant chemoattractant response range. It therefore seems that the intrinsic dynamic range of receptor activation is able to withstand wide variations in external attractant concentrations. In contrast, we cannot rule out that the lower cAR1 levels present in *pdsA*$^-$/PEC cells also account for the narrower range of responsiveness observed in these cells.

We discovered that the absence of PdsA dramatically alters the ability of cells to migrate in groups. Using the under-agarose assay, in which cell motion is restricted and the diffusion of large molecules, such as PdsA, is slowed (Johnson *et al.*, 1996), the *pdsA*$^-$/PEC cells migrated in a disordered manner, showing broad twisted streams as opposed to the single-file head-to-tail arrays observed in WT cells. In the needle assay, the external cAMP signal diffuses from a point source forming a radial gradient convergent at the needle. In this assay, WT cells formed clear, finely branched streams that dominated the field of view at high cell density. Alternatively, the migration behavior of *pdsA*$^-$/PEC cells showed a significant dependence on plating density. In addition, when streams formed they were not per-

sistent and favored cells traveling parallel to each other rather than in head-to-tail lines akin to what we observed with the under-agarose assay. Because we found that the absence of PdsA did not regulate the signal relay machinery (the extent and timing of the chemoattractant-mediated activation of ACA as well as the cellular distribution of ACA and CRAC were comparable to what is observed in WT cells), we conclude that the streaming defect we observed is associated with the effect of PdsA on the external cAMP gradient field. We speculate that without degradation, a local collection of cells produces more cAMP favoring the formation of thick aggregates. In WT cells, locally dense cell regions have a locally higher concentration of PdsA, making large clusters unfavorable.

We also found that the addition of exogenous PdsA dramatically disrupts the intrinsic ability of WT cells to stream and, most remarkably, it induced *pdsA*$^-$/PEC cells to migrate in groups and form streams. However, the migration behavior of the *pdsA*$^-$/PEC cells treated with PdsA was distinct from WT cells treated with PB. The streams in the treated *pdsA*$^-$/PEC cells were thicker and did not branch out to the extent that the WT cells did. It therefore seems that the addition of a bolus of PdsA is not optimal to induce normal streaming and branching. Using cell fractionation, it has been proposed that PdsA is present in both soluble and plasma membrane-bound forms (Malchow *et al*., 1972; Blondelet and Brachet, 1981; Bader *et al*., 2007). We now show that PdsA is not associated with the plasma membrane and that it is found exclusively on the ER. We presume that ER contamination in the plasma membrane fractions is responsible for the earlier findings. Because a uniform bolus of PdsA is not sufficient to fully restore the streaming ability of *pdsA*$^-$/PEC cells, we envision that a controlled and perhaps local secretion of the PdsA is involved. The secretion would be difficult to visualize. In fixed cells, secreted PdsA will be lost and with live cells, the YFP-PdsA is not expressed high enough to visualize. Furthermore, biochemical assays are not sensitive enough to detect PdsA secretion in a timely manner (Malchow *et al*., 1972). Nevertheless, we envision that coupled with the asymmetric distribution of ACA at the back of cells, this local pool of PdsA would ultimately favor migration in single-file lines.

Considering that the diffusion rate of cAMP is 2 orders of magnitude faster compared with the reported hydrolysis rate of cAMP by secreted PdsA (Gerisch, 1976; Nanjundiah and Malchow, 1976; Bader *et al*., 2007), our finding that only a soluble form of PdsA is available to degrade the cAMP signal and that its activity affects the shape of streams is surprising. Indeed, a computational investigation of the cAMP gradient field produced by signal relay determined that secreted PdsA does little to sharpen the gradient field and assist streaming (Tang and Othmer, 1995). Conversely, the activity of PdsA has been shown to be modulated by the presence of an inhibitor (PDI; phosphodiesterase inhibitor) that is expressed at different levels during development (Gerisch *et al*., 1972; Franke and Kessin, 1981), and when cells are pulsed with small amounts of cAMP (as in our study), the expression of the inhibitor is reduced and the activity of PdsA increases by ~2 orders of magnitude (Yeh *et al*., 1978). Under these conditions, our hypothesis that the secreted form of PdsA regulates cAMP gradients and group migration is more likely.

The transition of *Dictyostelium* from single to group cell behavior has been the subject of many modeling studies. In the majority of the papers published, cAMP is proposed to be uniformly emitted by cells in response to a cAMP signal, and the phosphodiesterase activity is either distributed uniformly extracellularly in space and time (Levine and Reynolds, 1991; Levine *et al*., 1996; Sawai *et al*., 2005), associated with the plasma membrane, or both (Pate and Odell, 1981; Tang and Othmer, 1995). Although both models are capable of reproducing many features of *Dictyostelium* aggregation, including the propagation of cAMP waves in characteristic spirals and the formation of stream-like aggregates, they are not perfect. In previous work, we have proposed that the secretion of cAMP is spatially restricted (Kriebel *et al*., 2003, 2008). We now show that only the secreted form of PdsA can degrade the external cAMP signal and that the addition of a uniform bolus of PdsA does not lead to the formation of highly branched, head-to-tail lines characteristic of WT streaming. It will therefore be interesting to see how including these new parameters improves the mathematical models that describe aggregation and streaming.

Although our study clearly defines an important role for extracellular chemoattractant degradation in the context of *Dictyostelium* chemotaxis and streaming, we envision that similar mechanisms are at play to regulate mammalian cell chemotaxis. In leukocyte migration and inflammation, a role for various proteases as well as internalization of bound receptor by decoy receptors has been suggested to remove attractant molecules and regulate chemoattractant gradients (Borroni *et al*., 2008; Friedl and Weigelin, 2008; Leung *et al*., 2008; Scola *et al*., 2008). Interestingly, the pathogenic bacteria *Pseudomonas aeruginosa* seems to use degradation of proinflammatory factors to prevent host defenses from fighting the infection (Leidal *et al*., 2003). In addition, *Drosophila* germ cell migration is negatively regulated by two lipid phosphatases (wunen and wunen-2) that are expressed by somatic cells. These phosphatases dephosphorylate lysophospholipids and provide repellent cues that steer the migrating cells toward the proper environment (Renault and Lehmann, 2006). In zebrafish development, germ cell migration is guided by the chemokine stromal cell-derived factor-1 (SDF-1). The CXCR4 receptor on migrating cells has been shown to guide their chemotaxis; however, mutations that control receptor internalization, and thereby signaling levels, have been shown to affect the precision of chemotaxis (Minina *et al*., 2007). In addition, CXCR7, which also binds SDF-1, is expressed in somatic tissue and seems to influence SDF-1 gradient formation by internalizing the attractant along the migration route (Boldajipour *et al*., 2008). It therefore seems that regulated attractant degradation allows a variety of cells to follow precise chemotactic path in complex environments.

ACKNOWLEDGMENTS

We thank Richard Kessin for providing the *pdsA*$^-$ cells. In addition, we thank the members of the Parent laboratory and the groups of Alan Kimmel, Tian Jin, and Wolfgang Losert for many helpful discussions and suggestions. This work was supported by the Intramural Research Program at the Center for Cancer Research, National Cancer Institute, National Institutes of Health and National Institute of Standards and Technology Center for Theoretical and Computational Materials Science grant 60NANB6D61200. E.C.R. is a recipient of a Career Award at the Scientific Interface from the Burroughs Wellcome fund.

REFERENCES

Aubry, L., and Firtel, R. (1999). Integration of signaling networks that regulate *Dictyostelium* differentiation. Annu. Rev. Cell Dev. Biol. *15*, 469–517.

Bader, S., Kortholt, A., and Van Haastert, P. J. (2007). Seven *Dictyostelium discoideum* phosphodiesterases degrade three pools of cAMP and cGMP. Biochem. J. *402*, 153–161.

Bagorda, A., Mihaylov, V. A., and Parent, C. A. (2006). Chemotaxis: moving forward and holding on to the past. Thromb. Haemost. *95*, 12–21.

Barra, J., Barrand, P., Blondelet, M. H., and Brachet, P. (1980). pdsA, a gene involved in the production of active phosphodiesterase during starvation of *Dictyostelium discoideum* amoebae. Mol. Gen. Genet. *177*, 607–613.

Blondelet, M. H., and Brachet, P. (1981). The hydrophobic character of the membrane-bound phosphodiesterase from *Dictyostelium discoideum*. Biochim. Biophys. Acta *640*, 572–582.

Boldajipour, B., Mahabaleshwar, H., Kardash, E., Reichman-Fried, M., Blaser, H., Minina, S., Wilson, D., Xu, Q., and Raz, E. (2008). Control of chemokine-guided cell migration by ligand sequestration. Cell *132*, 463–473.

Bolourani, P., Spiegelman, G. B., and Weeks, G. (2006). Delineation of the roles played by RasG and RasC in cAMP-dependent signal transduction during the early development of *Dictyostelium discoideum*. Mol. Biol. Cell *17*, 4543–4550.

Borroni, E. M., Bonecchi, R., Buracchi, C., Savino, B., Mantovani, A., and Locati, M. (2008). Chemokine decoy receptors: new players in reproductive immunology. Immunol. Invest. *37*, 483–497.

Brown, S. S., and Rutherford, C. L. (1980). Localization of cyclic nucleotide phosphodiesterase in the multicellular stages of *Dictyostelium discoideum*. Differentiation *16*, 173–183.

Chisholm, R. L., and Firtel, R. A. (2004). Insights into morphogenesis from a simple developmental system. Nat. Rev. Mol. Cell Biol. *5*, 531–541.

Comer, F. I., Lippincott, C. K., Masbad, J. J., and Parent, C. A. (2005). The PI3K-mediated activation of CRAC independently regulates adenylyl cyclase activation and chemotaxis. Curr. Biol. *15*, 134–139.

Comer, F. I., and Parent, C. A. (2006). Phosphoinositide 3-kinase activity controls the chemoattractant-mediated activation and adaptation of adenylyl cyclase. Mol. Biol. Cell *17*, 357–366.

Darmon, M., Barra, J., and Brachet, P. (1978). The role of phosphodiesterase in aggregation of *Dictyostelium discoideum*. J. Cell Sci. *31*, 233–243.

Devreotes, P. N. (1994). G protein-linked signaling pathways control the developmental program of *Dictyostelium*. Neuron *12*, 235–241.

Faure, M., Podgorski, G. J., Franke, J., and Kessin, R. H. (1988). Disruption of *Dictyostelium discoideum* morphogenesis by overproduction of cAMP phosphodiesterase. Proc. Natl. Acad. Sci. USA *85*, 8076–8080.

Faure, M., Podgorski, G. J., Franke, J., and Kessin, R. H. (1989). Rescue of a *Dictyostelium discoideum* mutant defective in cyclic nucleotide phosphodiesterase. Dev. Biol. *131*, 366–372.

Franke, J., and Kessin, R. H. (1981). The cyclic nucleotide phosphodiesterase inhibitory protein of *Dictyostelium discoideum*. Purification and characterization. J. Biol. Chem. *256*, 7628–7637.

Franke, J., and Kessin, R. H. (1992). The cyclic nucleotide phosphodiesterases of *Dictyostelium discoideum*: molecular genetics and biochemistry. Cell Signal. *4*, 471–478.

Friedl, P., and Weigelin, B. (2008). Interstitial leukocyte migration and immune function. Nat. Immunol. *9*, 960–969.

Garcia, G. L., and Parent, C. A. (2008). Signal relay during chemotaxis. J. Microsc. *231*, 529–534.

Gerisch, G. (1976). Extracellular cyclic-amp phosphodiesterase regulation in agar plate cultures of *Dictyostelium discoideum*. Cell Differ. *5*, 21–25.

Gerisch, G., Malchow, D., Riedel, V., Muller, E., and Every, M. (1972). Cyclic AMP phosphodiesterase and its inhibitor in slime mould development. Nat. New Biol. *235*, 90–92.

Hereld, D., Vaughan, R., Kim, J. Y., Borleis, J., and Devreotes, P. (1994). Localization of ligand-induced phosphorylation sites to serine clusters in the C-terminal domain of the *Dictyostelium* cAMP receptor, cAR1. J. Biol. Chem. *269*, 7036–7044.

Insall, R., and Andrew, N. (2007). Chemotaxis in *Dictyostelium*: how to walk straight using parallel pathways. Curr. Opin. Microbiol. *10*, 578–581.

Insall, R., Kuspa, A., Lilly, P. J., Shaulsky, G., Levin, L. R., Loomis, W. F., and Devreotes, P. (1994). CRAC, a cytosolic protein containing a pleckstrin homology domain, is required for receptor and G protein-mediated activation of adenylyl cyclase in *Dictyostelium*. J. Cell Biol. *126*, 1537–1545.

Janetopoulos, C., and Firtel, R. A. (2008). Directional sensing during chemotaxis. FEBS Lett. *582*, 2075–2085.

Janetopoulos, C., Jin, T., and Devreotes, P. (2001). Receptor-mediated activation of heterotrimeric G-proteins in living cells. Science *291*, 2408–2411.

Johnson, E. M., Berk, D. A., Jain, R. K., and Deen, W. M. (1996). Hindered diffusion in agarose gels: test of effective medium model. Biophys. J. *70*, 1017–1023.

Johnson, R. L., Vaughan, R. A., Caterina, M. J., Van Haastert, P. J., and Devreotes, P. N. (1991). Overexpression of the cAMP receptor 1 in growing *Dictyostelium* cells. Biochemistry *30*, 6982–6986.

Kay, R. R., Langridge, P., Traynor, D., and Hoeller, O. (2008). Changing directions in the study of chemotaxis. Nat. Rev. Mol. Cell Biol. *9*, 455–463.

Kolsch, V., Charest, P. G., and Firtel, R. A. (2008). The regulation of cell motility and chemotaxis by phospholipid signaling. J. Cell Sci. *121*, 551–559.

Kortholt, A., and van Haastert, P. J. (2008). Highlighting the role of Ras and Rap during *Dictyostelium* chemotaxis. Cell Signal *20*, 1415–1422.

Kriebel, P. W., Barr, V. A., and Parent, C. A. (2003). Adenylyl cyclase localization regulates streaming during chemotaxis. Cell *112*, 549–560.

Kriebel, P. W., Barr, V. A., Rericha, E. C., Zhang, G., and Parent, C. A. (2008). Collective cell migration requires vesicular trafficking for chemoattractant delivery at the trailing edge. J. Cell Biol. *183*, 949–961.

Lacombe, M. L., Podgorski, G. J., Franke, J., and Kessin, R. H. (1986). Molecular cloning and developmental expression of the cyclic nucleotide phosphodiesterase gene of *Dictyostelium discoideum*. J. Biol. Chem. *261*, 16811–16817.

Leidal, K. G., Munson, K. L., Johnson, M. C., and Denning, G. M. (2003). Metalloproteases from *Pseudomonas aeruginosa* degrade human RANTES, MCP-1, and ENA-78. J. Interferon Cytokine Res. *23*, 307–318.

Leung, L. L., Myles, T., Nishimura, T., Song, J. J., and Robinson, W. H. (2008). Regulation of tissue inflammation by thrombin-activatable carboxypeptidase B (or TAFI). Mol. Immunol. *45*, 4080–4083.

Levine, H., Aranson, I., Tsimring, L., and Truong, T. V. (1996). Positive genetic feedback governs cAMP spiral wave formation in *Dictyostelium*. Proc. Natl. Acad. Sci. USA *93*, 6382–6386.

Levine, H., and Reynolds, W. (1991). Streaming instability of aggregating slime mold amoebae. Phys. Rev. Lett. *66*, 2400–2403.

Mahadeo, D. C., and Parent, C. A. (2006). Signal relay during the life cycle of *Dictyostelium*. Curr. Top. Dev. Biol. *73*, 115–140.

Malchow, D., Nagele, B., Schwartz, H., and Gerisch, G. (1972). Membrane-bound cyclic AMP phosphodiesterase in chemotactically responding cells of *Dictyostelium discoideum*. Eur. J. Biochem. *28*, 136–142.

Manahan, C. L., Iglesias, P. A., Long, Y., and Devreotes, P. N. (2004). Chemoattractant signaling in *Dictyostelium discoideum*. Annu. Rev. Cell Dev. Biol. *20*, 223–253.

McMains, V. C., Liao, X. H., and Kimmel, A. R. (2008). Oscillatory signaling and network responses during the development of *Dictyostelium discoideum*. Ageing Res. Rev. *7*, 234–248.

Minina, S., Reichman-Fried, M., and Raz, E. (2007). Control of receptor internalization, signaling level, and precise arrival at the target in guided cell migration. Curr. Biol. *17*, 1164–1172.

Muller-Taubenberger, A., Lupas, A. N., Li, H. W., Ecke, M., Simmeth, E., and Gerisch, G. (2001). Calreticulin and calnexin in the endoplasmic reticulum are important for phagocytosis. EMBO J. *20*, 6772–6782.

Nanjundiah, V., and Malchow, D. (1976). A theoretical study of the effects of cyclic AMP phosphodiesterases during aggregation in *Dictyostelium*. J. Cell Sci. *22*, 49–58.

Orlow, S. J., Shapiro, I., Franke, J., and Kessin, R. H. (1981). The extracellular cyclic nucleotide phosphodiesterase of *Dictyostelium discoideum*. Purification and characterization. J. Biol. Chem. *256*, 7620–7627.

Pang, K. M., Lynes, M. A., and Knecht, D. A. (1999). Variables controlling the expression level of exogenous genes in *Dictyostelium*. Plasmid *41*, 187–197.

Parent, C. A., Blacklock, B. J., Froehlich, W. M., Murphy, D. B., and Devreotes, P. N. (1998). G protein signaling events are activated at the leading edge of chemotactic cells. Cell *95*, 81–91.

Parent, C. A., and Devreotes, P. N. (1995). Isolation of inactive and G protein-resistant adenylyl cyclase mutants using random mutagenesis. J. Biol. Chem. *270*, 22693–22696.

Parent, C. A., and Devreotes, P. N. (1996). Molecular genetics of signal transduction in *Dictyostelium*. Annu. Rev. Biochem. *65*, 411–440.

Pate, E. F., and Odell, G. M. (1981). A computer simulation of chemical signaling during the aggregation phase of *Dictyostelium discoideum*. J. Theor. Biol. *88*, 201–239.

Pitt, G. S., Milona, N., Borleis, J., Lin, K. C., Reed, R. R., and Devreotes, P. N. (1992). Structurally distinct and stage-specific adenylyl cyclase genes play different roles in *Dictyostelium* development. Cell *69*, 305–315.

Renault, A. D., and Lehmann, R. (2006). Follow the fatty brick road: lipid signaling in cell migration. Curr. Opin. Genet Dev. *16*, 348–354.

Sambrook, J. (2001). Molecular Cloning: A laboratory Manual, Cold Spring Harbor, NY: Cold Spring Harbor Laboratory Press.

Saran, S., Meima, M. E., Alvarez-Curto, E., Weening, K. E., Rozen, D. E., and Schaap, P. (2002). cAMP signaling in *Dictyostelium*—complexity of cAMP synthesis, degradation and detection. J. Muscle Res. Cell Motil. *23*, 793–802.

Sawai, S., Thomason, P. A., and Cox, E. C. (2005). An autoregulatory circuit for long-range self-organization in *Dictyostelium* cell populations. Nature *433*, 323–326.

Scola, A. M., Johswich, K. O., Morgan, B. P., Klos, A., and Monk, P. N. (2008). The human complement fragment receptor, C5L2, is a recycling decoy receptor. Mol. Immunol. *46*, 1149–1162.

Stephens, L., Milne, L., and Hawkins, P. (2008). Moving towards a better understanding of chemotaxis. Curr. Biol. *18*, R485–R494.

Sucgang, R., Weijer, C. J., Siegert, F., Franke, J., and Kessin, R. H. (1997). Null mutations of the *Dictyostelium* cyclic nucleotide phosphodiesterase gene block chemotactic cell movement in developing aggregates. Dev. Biol. *192*, 181–192.

Sussmann, M. (1966). Biochemical and genetic methods in the study of cellular slime mold development. In: Methods in Cell Physiology, vol. 2, ed. D. Prescott, New York: Academic Press, 397–410.

Tang, Y., and Othmer, H. G. (1995). Excitation, oscillations and wave propagation in a G-protein-based model of signal transduction in *Dictyostelium discoideum*. Philos. Trans. R. Soc. Lond. B Biol. Sci. *349*, 179–195.

Urushihara, H. (2008). Developmental biology of the social amoeba: history, current knowledge and prospects. Dev Growth Differ *50* (suppl 1), S277–S281.

van Haastert, P.J.M., and Devreotes, P. N. (2004). Chemotaxis: signalling the way forward. Nat. Rev. Mol. Cell. Biol. *5*, 626–634.

Van Lint, P., and Libert, C. (2007). Chemokine and cytokine processing by matrix metalloproteinases and its effect on leukocyte migration and inflammation. J. Leukoc. Biol. *82*, 1375–1381.

Weeks, G. (2000). Signalling molecules involved in cellular differentiation during *Dictyostelium* morphogenesis. Curr. Opin. Microbiol. *3*, 625–630.

Yamasaki, F., and Hayashi, H. (1982). Comparison of properties of the cellular and extracellular phosphodiesterases induced by cyclic adenosine 3′,5′-monophosphate in *Dictyostelium discoideum*. J. Biochem. *91*, 981–988.

Yeh, R. P., Chan, F. K., and Coukell, M. B. (1978). Independent regulation of the extracellular cyclic AMP phosphodiesterase-inhibitor system and membrane differentiation by exogenous cyclic AMP in *Dictyostelium discoideum*. Dev. Biol. *66*, 361–374.